


## Article

# Calculation of the Voltage Unbalance Factor for High-Speed Railway Substations with V-Connection Scheme

Didier Flumian \*, Philippe Ladoux \*  and Emmanuel Sarraute \*

LAPLACE, Université de Toulouse, CNRS, INPT, UPS, 31000 Toulouse, France

\* Correspondence: flumian@laplace.univ-tlse.fr (D.F.); ladoux@laplace.univ-tlse.fr (P.L.); sarraute@laplace.univ-tlse.fr (E.S.)

**Abstract:** In France, high-speed railway lines are powered by a  $2 \times 25$  kV/50 Hz electrification system. The substations include two single-phase transformers connected to the high-voltage electrical transmission network on different pairs of phases according to a so-called “V-connection scheme”. In practice, due to the large variations in the power absorbed by the trains, this connection does not make it possible to satisfactorily limit the unbalance in the three-phase voltages. In order to correctly size a balancing system to be associated with the substation, it is necessary to calculate, with precision, the voltage unbalance factor as a function of the power drawn by the trains. In its first part, this paper presents modelling of the substation and proposes an algorithm which allows for the calculation of the upstream line voltage as a function of the power consumption at the secondary of the transformers. The voltage unbalance factor can then be determined over a long period of operation. In the second part of this paper, the same approach is applied with an unbalance-compensator based on Steinmetz circuits controlled by AC choppers. Finally, in both cases, the results of the calculations are validated by simulations performed with PLECS simulation software.

**Keywords:** railway; traction substation; voltage unbalance factor; Steinmetz circuit; AC chopper



**Citation:** Flumian, D.; Ladoux, P.; Sarraute, E. Calculation of the Voltage Unbalance Factor for High-Speed Railway Substations with V-Connection Scheme. *Electronics* **2022**, *11*, 595. <https://doi.org/10.3390/electronics11040595>

Academic Editor: Francisco Gordillo

Received: 26 December 2021

Accepted: 12 February 2022

Published: 15 February 2022

**Publisher’s Note:** MDPI stays neutral with regard to jurisdictional claims in published maps and institutional affiliations.



**Copyright:** © 2022 by the authors. Licensee MDPI, Basel, Switzerland. This article is an open access article distributed under the terms and conditions of the Creative Commons Attribution (CC BY) license (<https://creativecommons.org/licenses/by/4.0/>).

## 1. Introduction

The “ $2 \times 25$  kV” railway electrification system was first used in 1972 on the Shinkansen Tokaido high-speed line in Japan, connecting the cities of Osaka and Yokohama [1]. In France, this power supply system was installed for the first time on the Paris–Lyon high-speed railway line in 1981 [2]. The principle, as presented in Figure 1, relies on a three-wire circuit: the substation utilizes a single-phase transformer with two secondary windings which supply the contact-line and a feed wire with voltages in phase-opposition. Autotransformers, regularly distributed along the line, boost the contact line voltage.

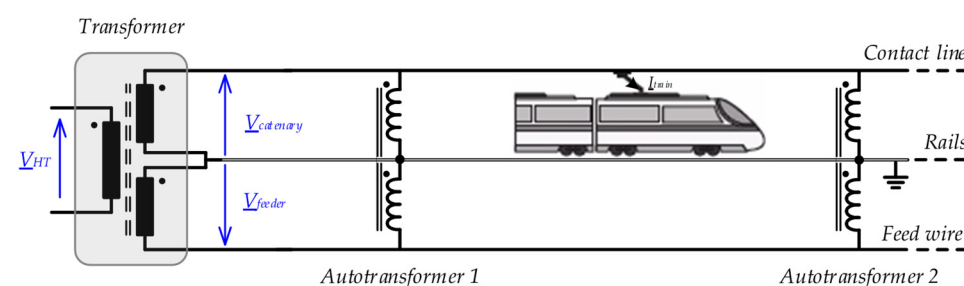


**Figure 1.** Principle of the “ $2 \times 25$  kV” railway electrification system.

When a train is located between two autotransformers, at the output of a substation, the current in the rails is canceled and the electrical power absorbed by the train is transmitted by both the contact line and feed wire at a voltage of 50 kV; this halves the currents circulating in the secondary windings of the transformer. Compared to the

classical two-wire 25 kV railway electrification system, the voltage drops and the Joule losses are lowered [3,4]. This is why the “ $2 \times 25$  kV” system is commonly used worldwide for supplying railway high-speed lines.

Due to the high-power supply of a high-speed line substation, it is also necessary to limit the voltage unbalance on the three-phase power grid. As shown in Figure 2, the substation uses a V-connection scheme with two single-phase transformers supplied by two line-to-line voltages. As a result, a neutral point is created at the substation and the power supply of the railway line is divided into two sectors.

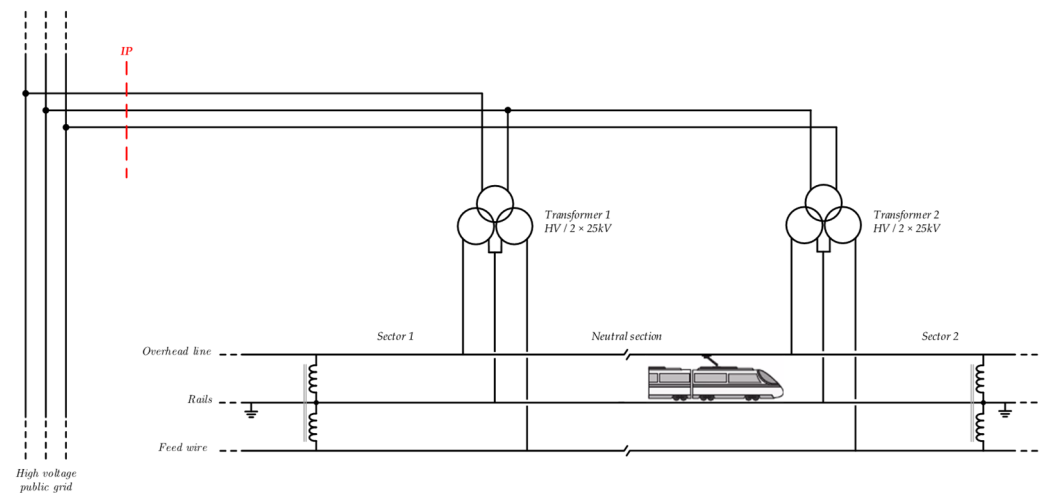


**Figure 2.** High-speed line substation with two transformers in “V-Connection”.

Usually, in V-connection substations, active and reactive power measurements are carried out at the secondary windings of the transformers. As a result, the primary winding currents are unknown and the calculation of the Voltage Unbalance Factor (VUF) at the Interconnection Point (IP) is an issue, as described in Section 2. Several authors have proposed empirical formulas intended to determine the unbalance factor using the apparent powers. However, as they do not consider separately the active and reactive powers, these calculations remain inaccurate [5–7]. Therefore, the first part of this paper presents an algorithm which allows for the line-to-line voltages at the input of the substation to be determined as a function of the power measurements provided by the remote metering system. Then, knowing the line-to-line voltages on the three-phase network, the VUF calculation is performed. A substation of the SNCF (French National Railways), located on the high-speed line between Paris and Strasbourg, has been considered as an application case. In the second part of the paper, the same algorithm is used to consider the connection of a voltage balancing system at the primary side of the substation. In all cases, the results of the calculation method are validated by simulations carried out with PLECS software [8].

## 2. Calculation Method for the Voltage Unbalance Factor

Nowadays, the SNCF traction substations are equipped with remote metering systems. At the request of the Transmission System Operator (TSO), the SNCF initiated a campaign to calculate the VUF at the connection points of traction substations. Active and reactive powers, averaged over 10 min, are stored and the number of events exceeding a 1% unbalance over a one-year period is recorded. In the future, substations whose VUFs regularly exceed 1% should be equipped with voltage balancing systems. The circuit presented in Figure 3 constitutes the basis of this study. The high-voltage electrical transmission network is modeled as an ideal three-phase voltage source with a positive phase-sequence, associated with a series RL circuit. The parameters of this impedance are calculated from the values of the short-circuit powers given by the TSO at the interconnection points of the traction substations. The transformers’ models include the turns ratios, the magnetizing inductances, the core-loss resistances, the leakage inductances, and the resistances of

each winding. These parameters are obtained from the data provided by the transformer manufacturer. The loads connected to the secondary windings of the two transformers are modeled by current sources operating at constant active and reactive powers. The powers (P and Q) correspond to those recorded by the remote metering systems.

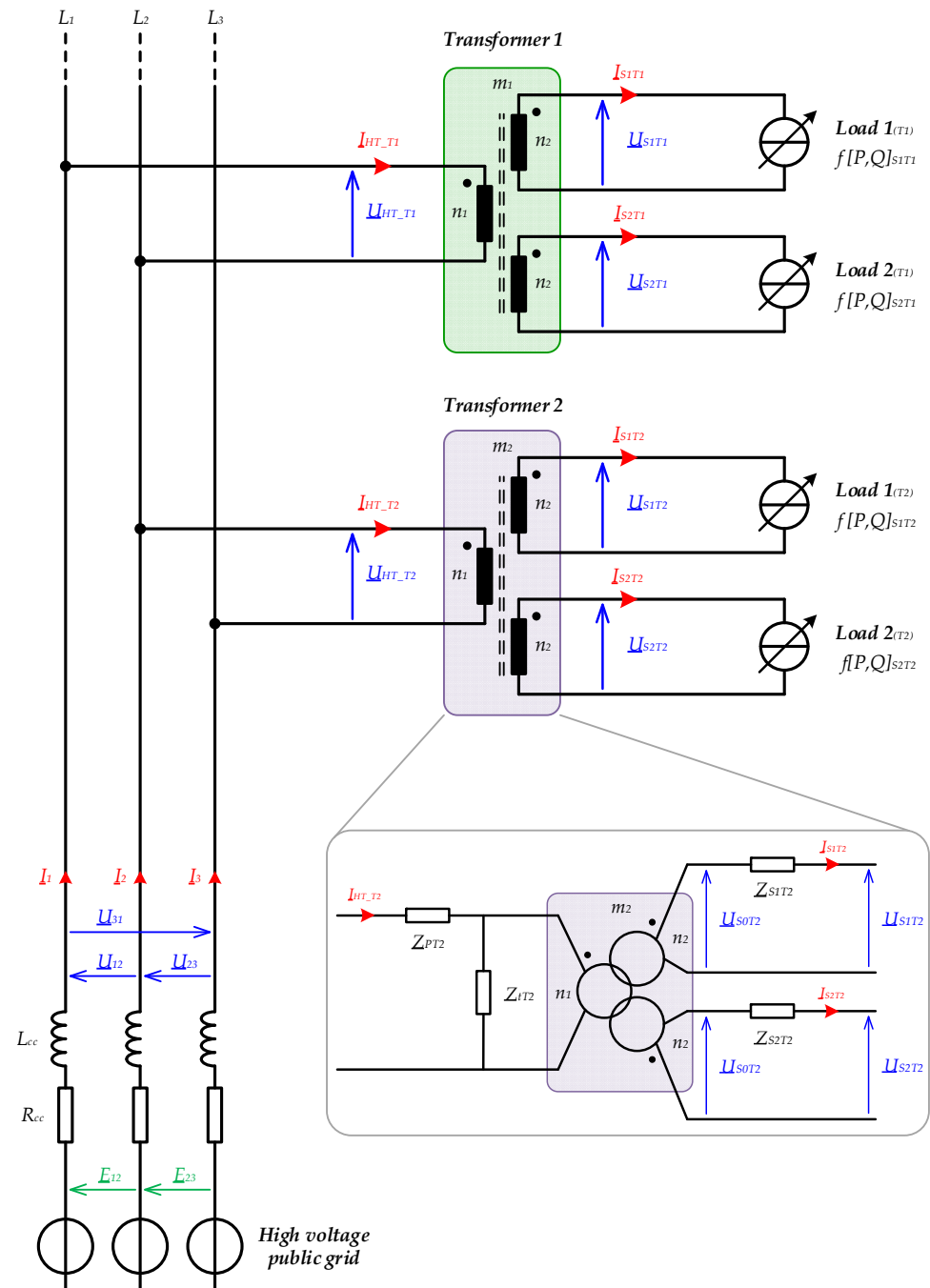


**Figure 3.** Diagram of the electrical circuit considered for the calculation of the VUF in the case of substations with V-connection schemes.

In order to determine the line-to-line voltages at the primary side of the two transformers and then to calculate the VUF, it is first necessary to determine the currents and voltages at the secondary side. Therefore, ten unknown complex quantities have to be determined:

- $\underline{U}_{S0T1}, \underline{U}_{S1T1}, \underline{I}_{S1T1}, \underline{U}_{S2T1}, \underline{I}_{S2T1}$  for Transformer 1; and
- $\underline{U}_{S0T2}, \underline{U}_{S1T2}, \underline{I}_{S1T2}, \underline{U}_{S2T2}, \underline{I}_{S2T2}$  for Transformer 2.

To determine these complex quantities, it is necessary to solve a system of ten equations with ten unknowns.

For Transformer 1, the following relationship between voltages and currents can be written from the circuit of Figure 3:

$$I_{HT\_T1} = m_1(I_{S1T1} + I_{S2T1}) + \frac{U_{S0T1}}{Z_{tT1} \cdot m_1} \quad (1)$$

with  $I_{HT\_T1}$  corresponding to the current at the primary side of Transformer 1.

$$U_{S0T1} = U_{S1T1} + Z_{S1T1} \cdot I_{S1T1} \quad (2)$$

For the first (“upper” in Figure 3) secondary side of Transformer 1.

$$U_{S0T1} = U_{S2T1} + Z_{S2T1} \cdot I_{S2T1} \quad (3)$$

For the lower secondary side of Transformer 1.

Similarly, the expressions for Transformer 2 are:

$$I_{HT\_T2} = m_2(I_{S1T2} + I_{S2T2}) + \frac{U_{S0T2}}{Z_{tT2} \cdot m_2} \quad (4)$$

with  $I_{HT\_T2}$  corresponding to the current at the primary side of Transformer 2.

$$U_{S0T2} = U_{S1T2} + Z_{S1T2} \cdot I_{S1T2} \quad (5)$$

For the upper secondary side of Transformer 2.

$$U_{S0T2} = U_{S2T2} + Z_{S2T2} \cdot I_{S2T2} \quad (6)$$

For the lower secondary side of Transformer 2.

The phase-to-phase voltages on the primary side are defined as:

$$U_{12} = E_{12} - Z_{cc}(2I_{HT\_T1} - I_{HT\_T2}) \quad (7)$$

and

$$U_{23} = E_{23} - Z_{cc}(2I_{HT\_T2} - I_{HT\_T1}) \quad (8)$$

Relations established from Kirchhoff’s laws should be completed by the complex apparent powers at each secondary winding of the transformers. The  $\underline{S}_{1T1}$ ,  $\underline{S}_{2T1}$ ,  $\underline{S}_{1T2}$ ,  $\underline{S}_{2T2}$  powers are directly calculated from the power measurements:

$$\underline{S}_{S1T1} = \underline{U}_{S1T1} \cdot I_{S1T1}^* = P_{S1T1} + jQ_{S1T1}$$

$$\underline{S}_{S2T1} = \underline{U}_{S2T1} \cdot I_{S2T1}^* = P_{S2T1} + jQ_{S2T1}$$

$$\underline{S}_{S1T2} = \underline{U}_{S1T2} \cdot I_{S1T2}^* = P_{S1T2} + jQ_{S1T2}$$

$$\underline{S}_{S2T2} = \underline{U}_{S2T2} \cdot I_{S2T2}^* = P_{S2T2} + jQ_{S2T2}$$

Then, the complex apparent powers, which are at the primary side of Transformers 1 and 2, can be calculated by Relations (9) and (10), respectively:

$$\begin{aligned} \underline{U}_{12} \times I_{HT\_T1}^* &= Z_{PT1} \times I_{HT\_T1}^2 + \frac{U_{S0T1}^2}{Z_{tT1}^* \times m_1^2} + Z_{S1T1} \times I_{S1T1}^2 + \underline{S}_{S1T1} \\ &\quad + Z_{S2T1} \times I_{S2T1}^2 + \underline{S}_{S2T1} \end{aligned} \quad (9)$$

where  $\underline{S}_{1T1}$  and  $\underline{S}_{2T1}$  are the complex apparent powers for both secondary windings of Transformer 1, determined from the power measurements:

$$\underline{U}_{23} \times \underline{I}_{HT\_T2}^* = \underline{Z}_{PT2} \times I_{HT\_T2}^2 + \frac{U_{S0T2}^2}{Z_{tT2}^* \times m_2^2} + \underline{Z}_{S1T2} \times I_{S1T2}^2 + \underline{S}_{S1T2} + \underline{Z}_{S2T2} \times I_{S2T2}^2 + \underline{S}_{S2T2}. \quad (10)$$

Expressions (1) to (10) correspond to a system of non-linear equations with ten complex electrical values. Indeed, the relations of the complex apparent powers involve products of voltage and current, which are unknown quantities. In this context, an iterative numerical method has been selected [9]. The principle of the method used is illustrated by Figure 4:

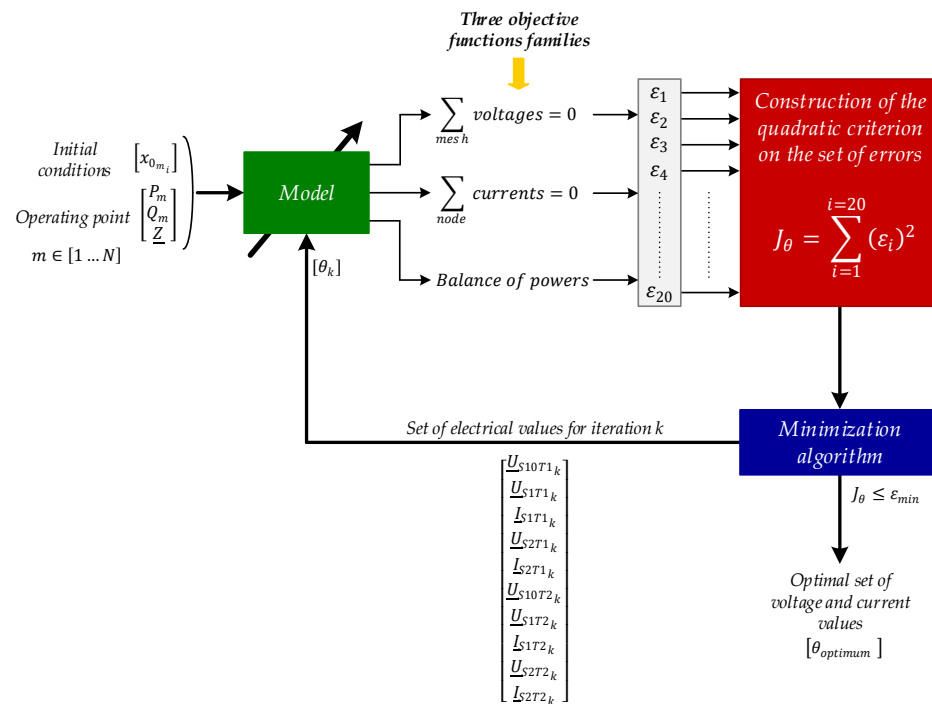


**Figure 4.** Principle for determining voltages and currents.

The Equations from (1) to (8) are written in a form that allows them to be solved by iterative methods: the sum of the voltages in a mesh is zero and the sum of the currents at a node is also zero. In addition, the power balance, given by Relations (9) and (10), completes the requirements of the objective functions that are used to search for the final (converged) set of voltage and current values.

### 2.1. Method Description

The iterative methods are based on the error calculation, which starts from an initial conditions vector  $[x_{0mi}]$  and which, by successive approaches, converges toward the solution for a given operating point. Therefore, they involve evolving the vector  $[\theta_k]$  to minimize an error criterion corresponding to the sum of the square of the errors. In other words, the objective of the method is to find the solution vector  $[\theta_{optimum}]$  such that the function  $J_\theta = f(\theta)$  is a minimum for that presented above. It is therefore an unconstrained optimization problem such as:

$$\min [J_\theta] = \min \sum_{i=1}^{i=20} (\epsilon_i)^2 \quad (11)$$

This technique is based on three important choices, which are as follows.

1. The initial conditions: A good knowledge of the initial conditions offers a reduced computation time (lower number of iterations, allowing for faster convergence towards a solution) and a better (more accurate) convergence. In the considered case, the initial conditions are calculated by determining the powers at the output of the transformers and neglecting the voltage drops in all the series impedances.
2. The recurrence method: Due to the non-linear nature of the model, the Levenberg-Marquardt algorithm has been used, which is a deterministic algorithm. This means that for the same starting point, the algorithm will always give the same result. It combines two algorithms: the gradient descent method when the observed values are “far” from the optimum (the first derivative is used) and the Gauss–Newton method when the observed values are close to the optimal solution (use of the second derivative). Thus, it is possible to ensure a more robust convergence with a low resolution time.
3. The stopping criterion: For the practical use of such a method, it is necessary to introduce a criterion to interrupt the iterative process when the approximation is judged “satisfactory”. For that, several choices are possible:
  - define a maximum number of iterations;
  - apply a tolerance  $\delta$  on the parameter’s increment (observation of two successive iterations); in this case, the iterations end when  $|\theta_k - \theta_{k+1}| \leq \delta$ ;
  - set a tolerance  $\varepsilon$  on the criterion of the objective function; in this case, the iterations end when  $|J_{\theta_k} - J_{\theta_{k+1}}| \leq \varepsilon$ ; and
  - apply a tolerance  $\mu$  on the gradient of the objective function  $J'_{\theta}$ ; the iterative process will then be interrupted when  $J'_{\theta} \leq \mu$ .

In our case, the  $\delta$ -stopping criteria have been attributed a value of  $1 \times 10^{-3}$ . This value reflects the relative tolerance accepted on the parameter’s evolution.

This method has been implemented in Matlab software and the results for a real case are presented in the next section.

## 2.2. Case Study

The SNCF has 47 substations with V-connections for more than 2800 km of high-speed lines. The traction substation located at “Trois Domaines” on the high-speed line between Paris and Strasbourg is considered as an application case (Table 1).

**Table 1.** “Trois domaines” substation characteristics.

Circuit Parameters	
Power supply voltage (kV)	225
Upstream network short-circuit power (MVA)	1304
Transformer power (MVA)	$2 \times 27.5$
Transformer 1 voltage ratio	0.122
Transformer 2 voltage ratio	0.122

### 2.2.1. Analysis of the Algorithm Operation for one Operating Point of the Substation

Active and reactive powers measured at the secondary sides of the two transformers are given in Table 2.

**Table 2.** Active and reactive power measurements.

Power	Transformer 1	Transformer 2
Active power Secondary 1 (MW)	3.29	11.34
Reactive power Secondary 1 (MVAR)	0.33	4.06
Active power Secondary 2 (MW)	2.54	7.68
Reactive power Secondary 2 (MVAR)	0.23	2.28

For this operating point, Table 3 summarizes the obtained results after running the Matlab calculation routine.

**Table 3.** Matlab calculation results.

Iteration	Residual
0	$1606 \times 10^{12}$
1	$4918 \times 10^9$
2	862,025
3	$^1 5835 \times 10^{-10}$

<sup>1</sup> Optimization stopped because the parameter's increment,  $\delta$ , is less than  $1 \times 10^{-3}$ .

Starting from the initial conditions (Iteration 0), the algorithm finds a solution and converges in three iterations, and the stopping criterion is the relative value of the parameter's evolution. The residual value corresponds to the square of the error of the objective function for each iteration, as follows:

$$Residual = \left( \sum J_{\theta}^2 \right)_k \quad (12)$$

The residual value of  $5835 \times 10^{-10}$  confirms the fact that the solver has converged to an acceptably accurate solution.

Figure 5 shows the evolution of the currents (real and imaginary parts) at the secondary side of the transformers according to the rank of the iterations. The solution found is close to the starting point, highlighting the importance of defining “good” initial conditions. From Iteration  $k = 1$ , the values evolve slightly, which leads to a fast convergence towards the solution.

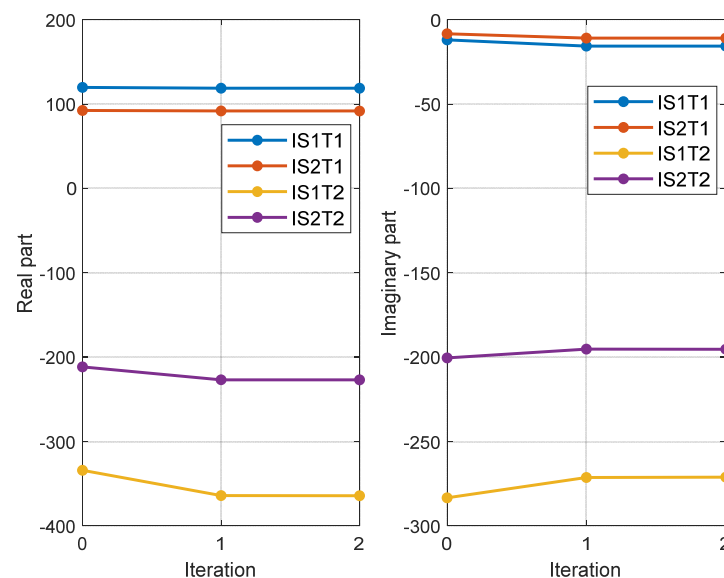


**Figure 5.** Secondary-side current values for each iteration. The voltage  $E_{12}$  is defined as the origin of the vectors in the complex reference frame.

### 2.2.2. Calculation of Voltage Unbalance Factor

Knowing the currents at the secondary side of the transformers, it is then possible to calculate the complex values of the currents and the voltages at the primary side of the substation. Using the Fortescue method [10,11], the symmetrical voltage components of the

positive and negative sequences of the three-phase voltage system at the interconnection point of the substation can be calculated according to Relations (13) and (14):

$$\underline{U}^+ = \frac{1}{3} (\underline{U}_{12} + a\underline{U}_{23} + a^2\underline{U}_{31}) \quad (13)$$

$$\underline{U}^- = \frac{1}{3} (\underline{U}_{12} + a^2\underline{U}_{23} + a\underline{U}_{31}) \quad (14)$$

where the complex operator 'a' is defined as  $a = e^{j\frac{2\pi}{3}}$ .

The voltage unbalance factor, also known as the "voltage asymmetry factor", is defined as the ratio of the negative and the positive sequence modulus:

$$VUF = \frac{|\underline{U}^-|}{|\underline{U}^+|} \quad (15)$$

For the considered operating point, the calculated unbalance factor is 1.55%.

### 2.2.3. Calculation of the VUF over a Long Period

The method previously presented is used to determine the evolution of the VUF over a one-year period. The calculation is carried out from average 10 min active and reactive power data recorded by the telemetry system; that is a total of 52,560 operating points to be considered per year. Figure 6 summarizes the number of operating points that exceed the 1% limit.

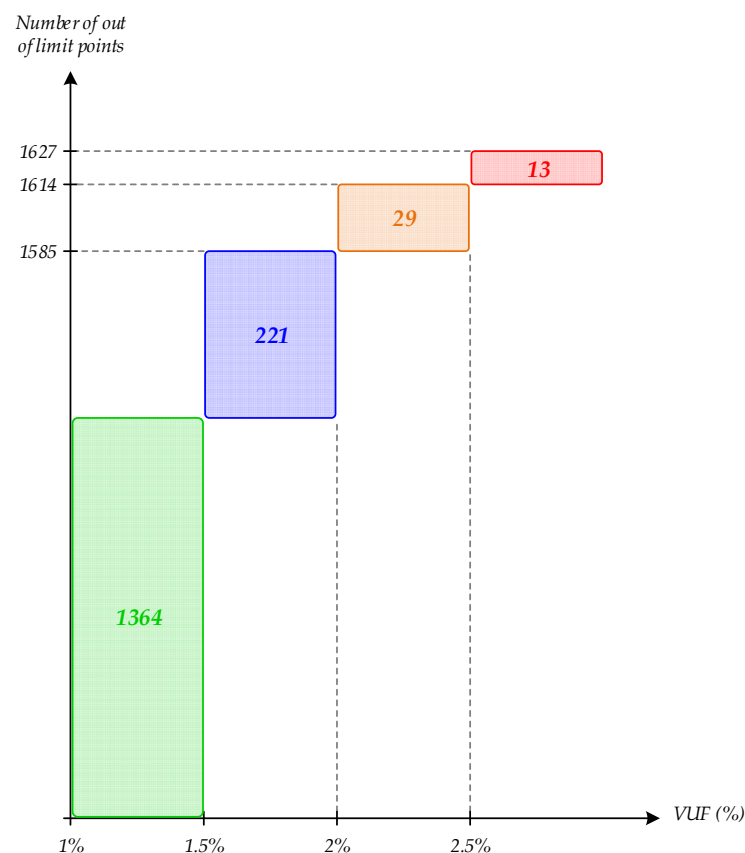


**Figure 6.** Number of out-of-limit operating points vs. VUF without balancing system over one year.

In principle, a VUF of higher than 1% is prohibited by the TSO. Nevertheless, a tolerance of a few tens of events over a year beyond this limit is accepted. Thus, the analysis of the calculation results clearly shows that the current situation is not acceptable and necessarily requires the installation of a balancing system.



### 3. Voltage Unbalance Calculation with the Compensation System Connected

There are mainly two voltage-balancer topologies: the voltage source inverter (VSI) [12–14] and the High Voltage Balancing System (HVBS). The second solution relies on a Steinmetz circuit and combines both inductors and capacitors whose impedances are continuously controlled by means of AC choppers [15]. This approach is more attractive than the inverter solution (VSI) due to lower losses in the power semiconductors and the smaller sizes of all passive components [16]. C.P. Steinmetz showed that the voltage unbalance caused by unbalanced currents can be eliminated by adding a symmetrization inductor and a symmetrization capacitor to the original circuit [17]. Figure 7 illustrates this principle for a resistive load connected across two lines. In this case, the three-phase currents  $I_1$ ,  $I_2$ ,  $I_3$  will be balanced as long as Relation (16) is satisfied.

$$L\omega = \frac{1}{C\omega} = R\sqrt{3} \quad (16)$$

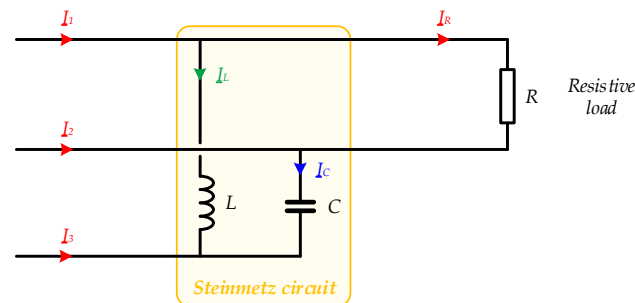


**Figure 7.** Basic principle of the Steinmetz balancing circuit.

Relation (16) can also be written in terms of the active power ( $P$ ) absorbed by the resistive load and the reactive powers in both inductor  $L$  and capacitor  $C$ :

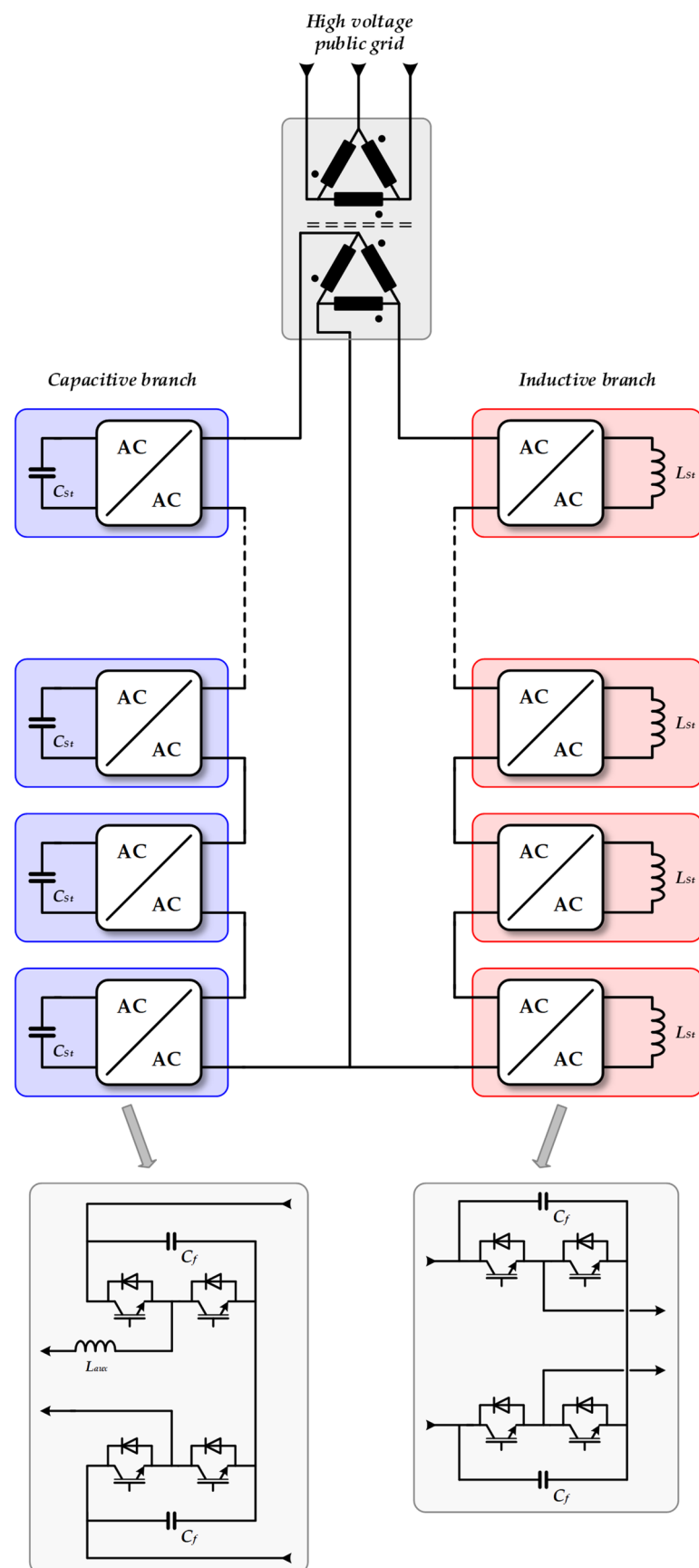
$$|Q_L| = |Q_C| = \frac{P}{\sqrt{3}} \quad (17)$$

For a variable resistive load, the reactive power in inductor  $L$  and capacitor  $C$  have to be adjusted. In the case of a single-phase traction substation, the balancing circuit is composed of two branches (i.e., inductive and capacitive branches) with several AC choppers connected in series, according to Figure 8. A three-phase transformer is used to stepdown the voltage level. The duty cycle “ $\alpha$ ” of the AC choppers is then controlled according to Relation (18), where  $P$  is the active power absorbed by the load (i.e., the trains) and  $Q_X$  is the maximum reactive power in the inductive and capacitive branches:

$$\alpha^2 = \frac{P}{\sqrt{3} \cdot Q_X} \quad (18)$$

The main characteristics of this compensation system are summarized in Table 4.

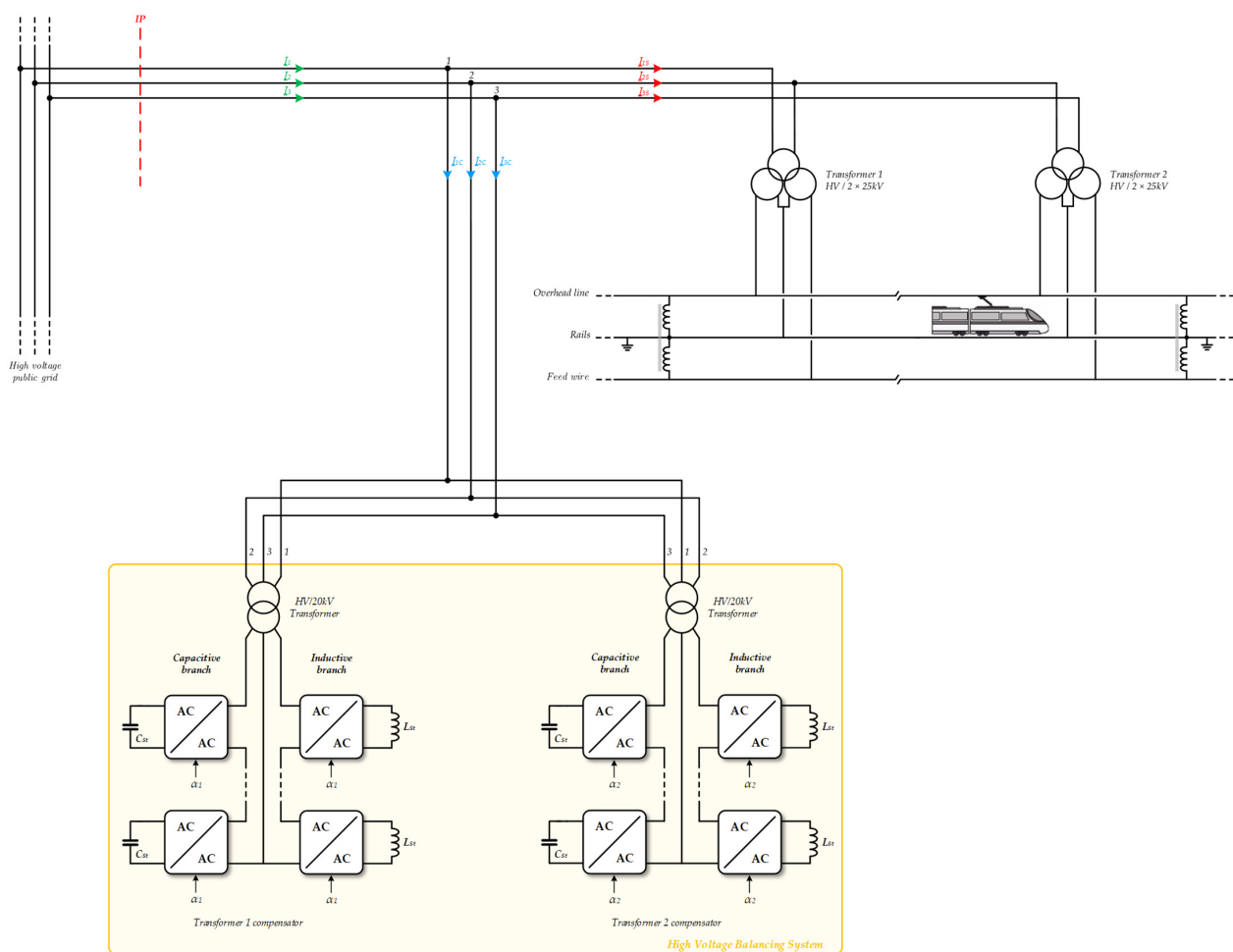
In the case of a substation using a V-connection, the High Voltage Balancing System (HVBS) has to include an active Steinmetz circuit for each transformer. The connection is given in Figure 9.



**Figure 8.** Topology of the active Steinmetz balancing system.

**Table 4.** Characteristics of the voltage balancer based on the Steinmetz circuit controlled by AC choppers.

Parameters	Values
Transformer nominal power, $S_n$ (MVA)	7
Turns ratio (20 kV/225 kV)	0.08
Nominal reactive power per branch, $Q_x$ (MVAR)	3.3
Number of AC choppers in series	36
IGBT collector-emitter voltage, $V_{CES}$ (V)	1700
IGBT DC collector current, $I_C$ (A)	450
Switching frequency (kHz)	18
Inductive branch inductor $L_{St}$ (mH)	9.75
Capacitive branch auxiliary inductor $L_{aux}$ (mH)	2.4
Capacitive branch capacitor $C_{St}$ ( $\mu$ F)	750
Input filter capacitor $C_f$ ( $\mu$ F)	22

**Figure 9.** Implementation of the High Voltage Balancing System in a substation with a V-connection scheme.

To take into account the influence of the HVBS on the VUF, the averaged model of the AC choppers was considered. Thus, the inductive and capacitive branches are modeled by two variable complex impedances, namely  $\underline{Z}_L$  and  $\underline{Z}_C$ , which depend on the duty cycles  $\alpha_1$  and  $\alpha_2$ . The control of the balancing system is very simple: the duty cycle of each active Steinmetz circuit is fixed according to the total active power delivered by the corresponding transformers:

$$\alpha_1^2 = \frac{P_{S1T1} + P_{S2T1}}{\sqrt{3} \cdot Q_X} \quad (19)$$

and

$$\alpha_2^2 = \frac{P_{S1T2} + P_{S2T2}}{\sqrt{3} \cdot Q_X} \quad (20)$$

Figure 10 illustrates the final circuit, which is considered to establish the new equations of the electrical circuit.

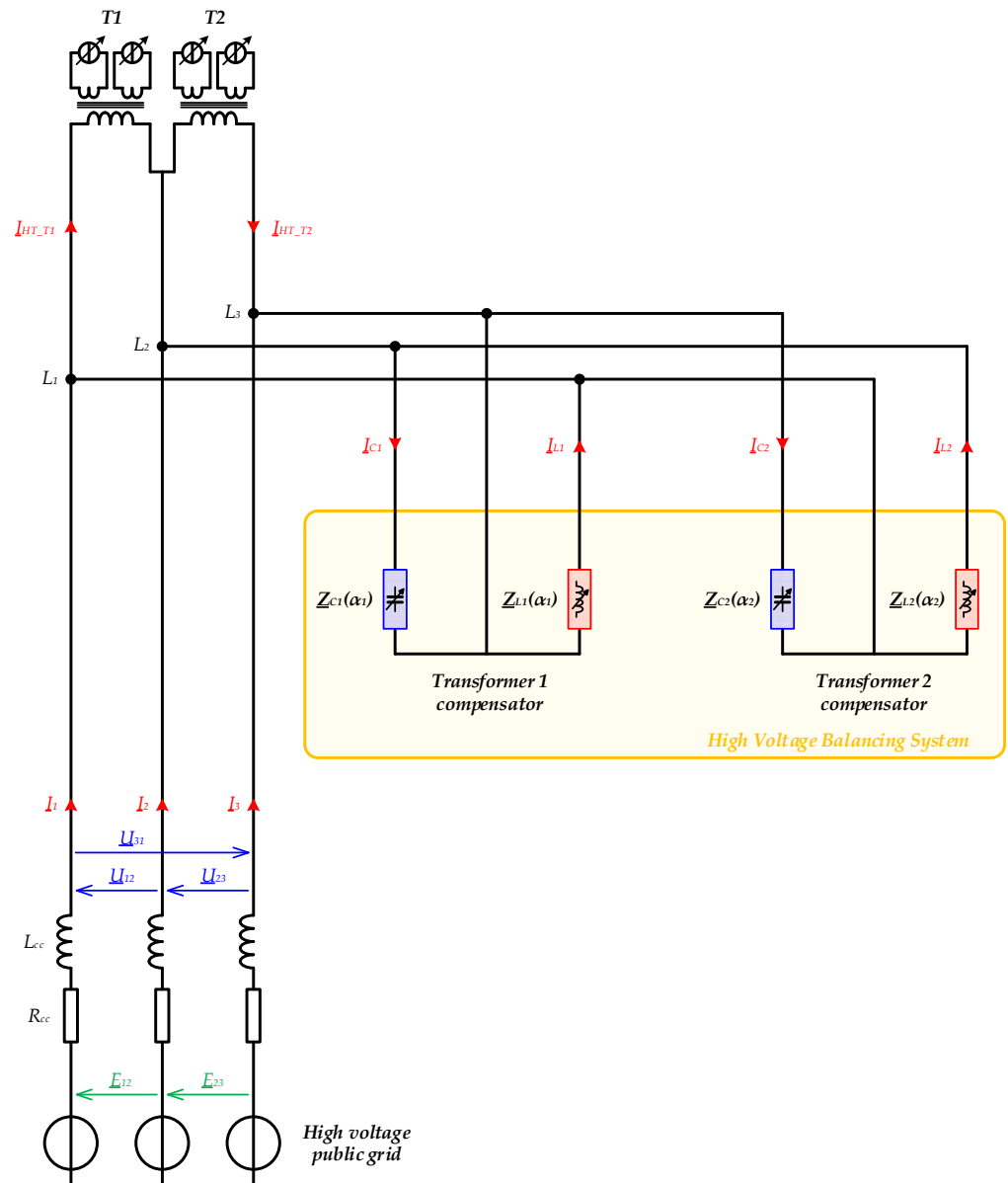


**Figure 10.** Equivalent circuit of the substation with the HVBS connected.

With this new configuration, Equations (7) and (8), which express the phase-to-phase voltages, become:

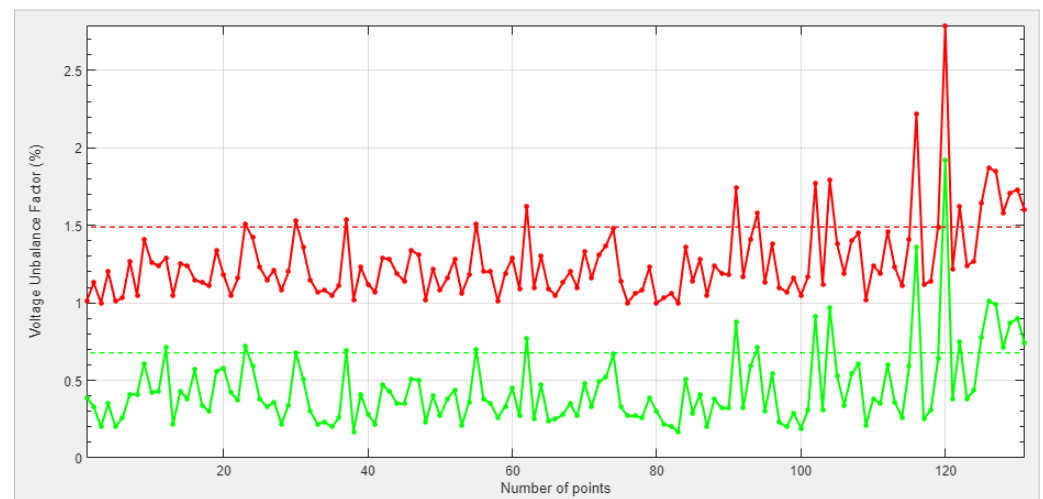
$$U_{12} = E_{12} - Z_{cc} \left( 2I_{HT-T1} - I_{HT-T2} + U_{12} \left( \frac{1}{Z_{L1}} + \frac{2}{Z_{L2}} + \frac{1}{Z_{C2}} \right) + U_{23} \left( \frac{1}{Z_{L1}} - \frac{1}{Z_{C1}} + \frac{1}{Z_{C2}} \right) \right) \quad (21)$$

and

$$\underline{U}_{23} = \underline{E}_{23} - \underline{Z}_{cc} \left( 2I_{HT\_T2} - I_{HT\_T1} + \underline{U}_{12} \left( \frac{1}{\underline{Z}_{L1}} - \frac{1}{\underline{Z}_{L2}} + \frac{1}{\underline{Z}_{C2}} \right) + \underline{U}_{23} \left( \frac{1}{\underline{Z}_{L1}} + \frac{2}{\underline{Z}_{C1}} + \frac{1}{\underline{Z}_{C2}} \right) \right) \quad (22)$$

These two expressions form a system of two equations with two unknown variables that can be solved numerically and thus the calculation of VUF is carried out in the same way as in Section 2.2.2.

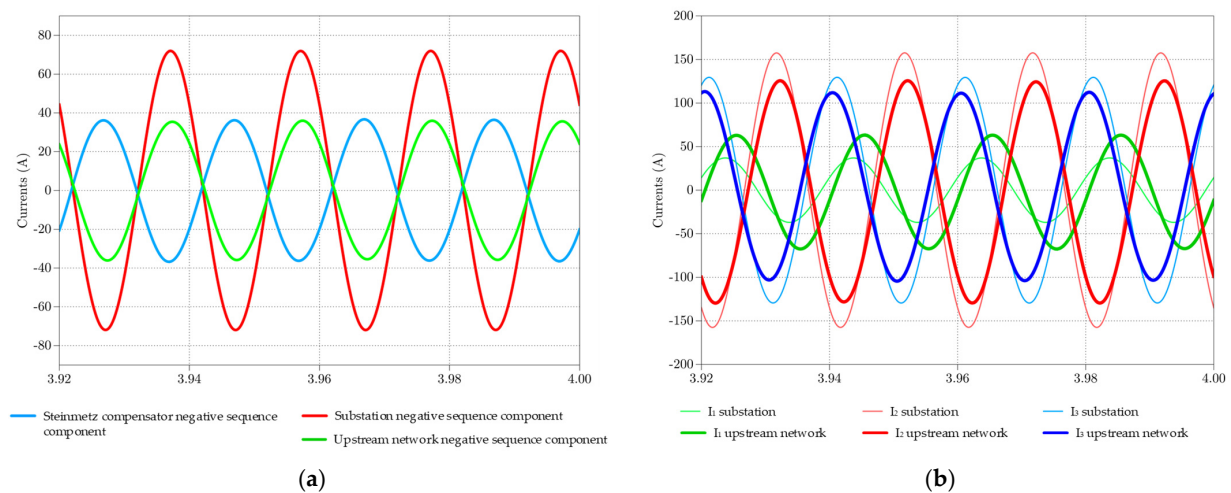
According to the power consumption of the traction substation located at “Trois Domaines”, the calculation results showed that it is necessary to install two HVBS in parallel in order to bring the VUF to a maximum value of around 1%. Figure 11 gives the result of an analysis over a one-month period considering the measurements of active and reactive powers averaged over 10 min, which represents 4320 points. Before compensation, 131 points are beyond 1% and only three points after compensation. Considering a period of one year, 1627 operating points out of 52,560 were over the 1% limit. With two HVBS connected in parallel, only 69 operating points exceed 1% and the averaged value of VUF over one year is 0.53%, which is perfectly tolerable for the TSO.



**Figure 11.** Data analysis over a one-month period: the red curve represents the voltage unbalance factor without compensation and the green curve represents the voltage unbalance factor with two Steinmetz active compensators connected.

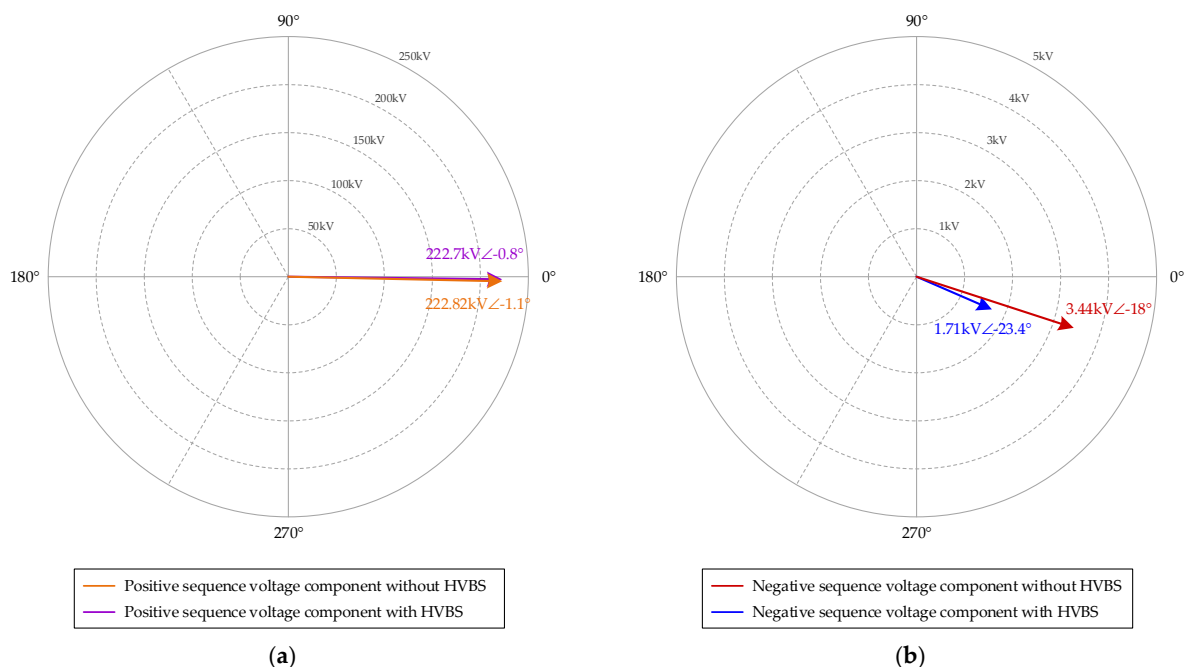
The entire circuit, including the two HVBSs, was implemented in PLECS software using the averaged model of the AC choppers [18]. To illustrate the calculation results, simulations were performed for the operating point presented in Table 2.

Figure 12a shows the negative sequence components of the three-phase currents at different points of the circuit. The HVBS absorbs a negative sequence current in phase-opposition with that of the substation. The negative sequence current at the point of interconnection is halved, which is enough to bring the VUF back below 1%. Figure 12b shows the three-phase current waveforms at the substation and at the interconnection point. Specifically, these waveforms highlight the fact that the HVBS rebalances the magnitude and the phase of the three-phase currents at the interconnection point.



**Figure 12.** (a) Negative sequence currents. (b) Substation currents (primary of both transformers T1 and T2) and upstream network currents.

The simulations show the effect of the HVBS on the VUF. Figure 13 shows, in the complex plane, the positive and negative sequence voltages before and after compensation. Phase-to-phase voltage  $E_{12}$  is the reference of  $E_{12} = E_{12}e^{-j0}$ . The negative sequence voltage is decreased by 50% and the VUF goes from 1.55% to 0.77%. The simulation results also confirm the validity of the calculation method proposed in Section 2. As a comparison, considering the same operating point, the empirical formulas presented in papers [5,6] give, respectively, a value of the unbalance factor of 1.34% and 1.37%, i.e., a relative error of 13.5% and 11.7%. It should be noted that these formulas cannot be used with a balancing system.



**Figure 13.** (a) Vector diagram of positive-sequence voltages. (b) Vector diagram of negative-sequence voltages.

#### 4. Conclusions

The calculation method presented in this paper makes it possible to accurately determine, from power telemetry, the VUF for traction substations with V-connection schemes. The processing of the 52,560 points corresponding to a year's operation was carried out in

1.5 h on a desktop computer. It moves away from empirical methods which are still used in practice.

- A complete modelling of the substation, including the transformers and the upstream electric network, was proposed.
- An iterative algorithm was proposed for solving the circuit equations. Once all the electrical quantities have been calculated, it is possible to determine the VUF at the connection point of the substation.
- In Section 3, the circuit equations were easily modified to include a balancing system based on a Steinmetz circuit controlled by AC choppers and the same iterative algorithm was used.

In all cases, the results obtained from the iterative calculation method were compared with simulations carried out with PLECS power electronic circuit simulation software. The error on all voltage and current quantities always remains as less than 1%. Finally, the calculation tool presented in this paper is essential for a railway network operator. On the one hand, it allows for the determination of the VUF from the power consumption of a substation and, on the other hand, it makes it possible to analyze the effect of installing a balancing system based on a Steinmetz circuit controlled by AC choppers.

**Author Contributions:** Methodology, P.L. and D.F.; software, D.F.; validation, P.L.; writing—original draft preparation, D.F.; writing—review and editing, D.F., P.L. and E.S. All authors have read and agreed to the published version of the manuscript.

**Funding:** This work was supported by ADEME (French Agency for Ecological Transition) in the frame of the HVBS (High Voltage Balancing System) project. URL: <https://librairie.ademe.fr/recherche-et-innovation/579-hvbs-high-voltage-balancing-system.html> (accessed on 2 February 2022).

**Data Availability Statement:** The data presented in this study are available upon request from the corresponding author.

**Conflicts of Interest:** The authors declare no conflict of interest.

## Abbreviations

The following abbreviations are used in this paper:

$U, I$	voltage and current modulus
$\underline{U}, \underline{I}$	complex voltage and current
$\underline{U}^*, \underline{I}^*$	conjugate complex voltage and current
$\underline{S}$	complex apparent power
$\underline{Z}$	complex impedance
$\varepsilon$	error

## References

1. Everett, A. Electric railway traction. *J. Inst. Electr. Eng.* **1919**, *57*, 312–316. [CrossRef]
2. Courtois, C. Why the  $2 \times 25$  kV alternative? (autotransformer traction supply). In Proceedings of the IEE Colloquium on 50 kV Autotransformer Traction Supply Systems—The French Experience, London, UK, 9 November 1993; pp. 111–114.
3. Roussel, H. Power Supply for the Atlantic TGV High Speed Line. In Proceedings of the International Conference on Main Line Railway Electrification 1989, York, UK, 25–28 September 1989; pp. 388–392.
4. Plakhova, M.; Mohamed, B.; Arboleya, P. Static model of a  $2 \times 25$  kV AC traction system. In Proceedings of the 2015 6th International Conference on Power Electronics Systems and Applications (PESA), Hong Kong, China, 15–17 December 2015. [CrossRef]
5. Chen, T.-H. Criteria to estimate the voltage unbalances due to high-speed railway demands. *IEEE Trans. Power Syst.* **1994**, *9*, 1672–1678. [CrossRef]
6. Kuo, H.-Y.; Chen, T.-H. Rigorous evaluation of the voltage unbalance due to high-speed railway demands. *IEEE Trans. Veh. Technol.* **1998**, *47*, 1385–1389. [CrossRef]
7. Golovanov, N.; Lazaroiu, G.; Roscia, M.; Zaninelli, D. Voltage unbalance vulnerability areas in power systems supplying high speed railway. In Proceedings of the IEEE Power Engineering Society General Meeting, 2005, San Francisco, CA, USA, 16 June 2005; Volume 3, pp. 2509–2514. [CrossRef]
8. Plexim, “PLECS”. Available online: <https://www.plexim.com/> (accessed on 2 February 2022).

9. López, C.P. *MATLAB Optimization Techniques*; Apress Academic; Springer: New York, NY, USA, 2005.
10. Fortescue, C.L. Method of symmetrical coordinates applied to solution of poly-phase networks. In Proceedings of the 34th Convention of American Institute of Electrical Engineers, Atlantic City, NJ, USA, 28 June 1918; Volume 37, pp. 1027–1140. [\[CrossRef\]](#)
11. Manesse, G. Transformateurs statiques Principes et fonctionnement. *Tech. L'ingénieur Convers. L'énergie Électrique* **2000**, 1–48. [\[CrossRef\]](#)
12. Aeberhard, M.; Courtois, C.; Ladoux, P. Railway traction power supply from the state of the art to future trends. In Proceedings of the International Symposium on Power Electronics, Electrical Drives, Automation and Motion, SPEEDAM 2010, Pisa, Italy, 14–16 June 2010; pp. 1350–1355. [\[CrossRef\]](#)
13. Moriyama, H.; Shimizu, T.; Kai, M.; Kunomura, K. Integrating the system of the electric power compensators for the Tokaido Shinkansen. In Proceedings of the 12th World Congress on Railway Research, Tokyo, Japan, 28 October–1 November 2019; pp. 1–6.
14. Tanta, M.; Pinto, J.G.; Monteiro, V.; Martins, A.P.; Carvalho, A.S.; Afonso, J.L. Topologies and Operation Modes of Rail Power Conditioners in AC Traction Grids: Review and Comprehensive Comparison. *Energies* **2020**, *13*, 2151. [\[CrossRef\]](#)
15. Ladoux, P.; Raimondo, G.; Caron, H.; Marino, P. Chopper-Controlled Steinmetz Circuit for Voltage Balancing in Railway Substations. *IEEE Trans. Power Electron.* **2013**, *28*, 5813–5822. [\[CrossRef\]](#)
16. Ladoux, P.; Fabre, J.; Caron, H. Power Quality Improvement in ac Railway Substations: The concept of chopper-controlled impedance. *IEEE Electr. Mag.* **2014**, *2*, 6–15. [\[CrossRef\]](#)
17. Harmon, P.; Lavers, J. A novel continuously variable single to three phase load matching circuit. *IEEE Trans. Magn.* **1982**, *18*, 1749–1751. [\[CrossRef\]](#)
18. Ladoux, P.; Chéron, Y.; Lowinsky, A.; Raimondo, G.; Marino, P. New Topologies for Static Reactive Power Compensator Based on PWM AC Choppers. *EPE J.* **2011**, *21*, 22–32. [\[CrossRef\]](#)